Contents

1 Introduction **3**

2 Differential Cross Section **3**

3 Reference Frames **4**

4 Coulomb Scattering **4**
4.1 General case 4
4.2 Rutherford scattering 5
4.2.1 Experimental considerations 6
4.2.2 Projectile beam with constant velocity 6
4.2.3 Projectile beam with Gaussian velocity distribution 7

5 Incorporating wave nature of particles **7**

6 Scattering Amplitude and Form Factor **8**

7 Fundamental Forces **10**
7.1 Gravitational and electromagnetic forces 10
7.2 Weak nuclear force 10
7.3 Strong nuclear force 10

8 Phases of Matter and Phase Transitions **11**
8.1 Phase diagrams 11
8.2 Order parameter 12
8.3 Classifications of phase transitions 12

9 Quark-Gluon Plasma **13**
9.1 Introduction 13
9.2 Phase transition from hadronic phase to QGP 14
9.3 Experimental detection of QGP 15
9.3.1 Jet Quenching 15
9.3.2 Elliptic Flow 16
9.4 Chiral symmetry breaking 16

10 Conclusion **17**

List of Tables

1 Wavelengths of particles for different energies 9

List of Figures

1 Collision in the CM frame. v_0 is the initial relative velocity (and final). 5
2 Scattering of reduced mass particle from a fixed centre of force 5
3 Variation of y vs θ with projectile and target properties 6
4 Dependence of y on the properties of velocity distribution of incident beam . . 8
5 Phase diagram of water [9] 11
6 Phase diagram of nuclear matter [9] 13

7 Plot of collision energies vs temperature of out-going hadrons [10] 14
8 Figure depicting a peripheral collision which shows the participants (interacting nucleons) in red and spectators (non-interacting nucleons) in blue. The reaction plane is the x-z plane in the diagram, which is formed by the impact parameter and the beam direction. [13] 16

Rutherford Scattering and its Applications in High Energy Nuclear Physics

1 Introduction

The quark-gluon plasma is a phase of matter thought to have existed in the early stages of evolution of the universe, and understanding this elusive form of matter has garnered great interest in recent years. The biggest and most technologically advanced machines that we have ever built are currently being used to create and study QGP in laboratories such as the European Organization for Nuclear Research (CERN). In this study, an attempt is made to understand the nature and properties of QGP from a practical and experimental perspective, with a special emphasis on how is it that we know what we know. Also, we start by taking a quick look at scattering experiments and their analysis, for these form the basis for the modern high energy experiments that look for QGP. The goal of the study is not to be mathematically rigorous, but to provide physical insight into the various phenomena that have been looked at.

2 Differential Cross Section

The primary output variable that we are concerned with in a scattering experiment is the differential cross section, which is a quantity that is directly proportional to the number of incident particles scattered at a given angle. By definition, the cross section (total) σ, for a collision process when a projectile is passing through a target with particle density n is such that the number of such collisions per unit path length is $n\sigma$ [1] .The differential cross-section can also be understood as the area on which the projectile has to be incident on to get scattered into unit solid angle at a particular scattering angle θ. It depends on the impact parameter b of the collision, which is the closest distance at which the projectile and target particles pass by each other if they don't interact. We shall work with the assumption that for a given pair of projectile and target particles with all properties fixed except the impact parameter, there is a single and unique scattering angle for each impact parameter.

Suppose that for the incoming particle to get scattered into an angle between θ and $\theta - d\theta$, the impact parameter of the collision should lie between b and $b + db$. Here we've utilised the fact that as the impact parameter increases, the scattering angle decreases for a central force which falls off with distance. Then the cross section $d\sigma$ is given by

$$d\sigma = 2\pi b \cdot db$$

$$\frac{d\sigma}{d\theta} = 2\pi b \frac{db}{d\theta}$$

where θ is the scattering angle. In terms of solid ange Ω, it can be written as

$$\frac{d\sigma}{d\Omega} = \frac{b}{\sin\theta} \left| \frac{db}{d\theta} \right| \tag{1}$$

This is the general equation for the differential cross-section [2], irrespective of the type of scattering. The modulus was introduced because $db/d\theta$ is negative, but we would like the differential cross section to be a positive quantity to give it a meaningful interpretation. In this equation, we substitute an expression for b in terms of θ to yield the differential cross-section as a function of the scattering angle.

3 Reference Frames

When studying collisions, there are two reference frames of interest, which are the lab and the centre of mass (CM) frames. The scattering angle for the projectile is different for the two frames, and are connected by the equation

$$\cot \chi_L = \frac{V}{v_0} \frac{m_1 + m_2}{m_2} \csc \chi_c + \cot \chi_c \tag{2}$$

which is obtained by exploiting the relation between the velocities of the particles in the lab and CM frames [3]. χ_L is the scattering angle in the lab frame, χ_c is the scattering angle in the centre of mass frame, V is the velocity of the centre of mass in the lab frame, v_0 is the initial relative velocity of the projectile and the target, m_1 is the mass of the projectile and m_2 is the mass of the target. If $\alpha = \frac{V}{v_0}\frac{m_1+m_2}{m_2}$, then the equation can be written in a simplified form as

$$\tan \chi_L = \frac{\sin \chi_c}{\alpha + \cos \chi_c}$$

4 Coulomb Scattering

Coulomb scattering refers to the scattering of charged particles which interact via coulomb interaction. In this study, we'll be concerned with two-particle elastic scattering (which involves a projectile and a target), where there are no energy losses in the form internal excitation of the colliding particles or the creation of new particles. We'll first look at the general case where the projectile and target have finite velocities and masses, and then move on to Rutherford's scattering experiment, which is a special (and simpler) case of coulomb scattering. It is to be noted that what follows is a classical treatment of the problem without taking relativistic effects or wave nature of particles into consideration, and both the projectile and target shall be taken to be point charges unless otherwise stated.

4.1 General case

Let the masses, charges, position vectors and initial velocities of the particles be given by $m_i, q_i, \vec{r_i}$ and $\vec{v_i}$ respectively where the index of the projectile is 1 and that of the target is 2.

As this is a two-particle collision, the problem can be made easier to solve using the reduced mass technique, considering a single particle of mass $\mu = \frac{m_1 m_2}{m_1+m_2}$ and position vector $\vec{r} = \vec{r_1} - \vec{r_2}$ with respect to a fixed centre of force (depicted in figure 2). The scattering angle so obtained is the same as the scattering angle in the CM frame. This is because since the momentum of the particles are equal and opposite at all times in the CM frame, the scattering angle of the incident (and target) particle will be equal to the final angle of the relative position vector $\vec{r}$. The schemtaic diagram is given in figure 1.

Using the laws of conservation of energy and angular momentum, the trajectory of this particle can be solved (and is found to be a parabola) [2], and its scattering angle θ is given in terms of its impact parameter b by the equation

$$\cot(\frac{\theta}{2}) = \frac{b}{a} \tag{3}$$

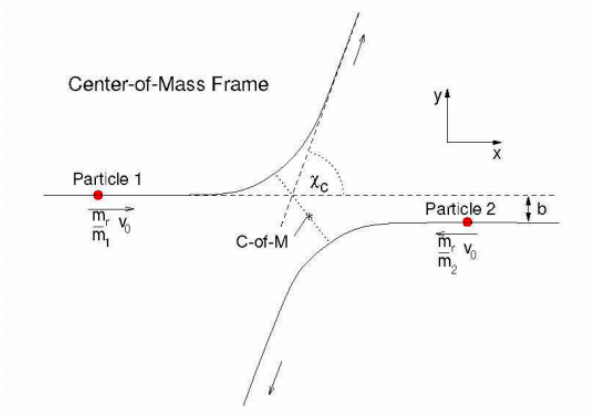

Figure 1: Collision in the CM frame. v_0 is the initial relative velocity (and final).

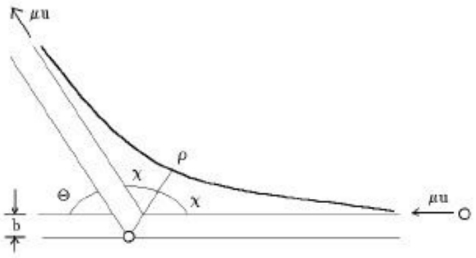

Figure 2: Scattering of reduced mass particle from a fixed centre of force

with

$$a = \frac{q_1 q_2}{4\pi\epsilon_0}\frac{1}{\mu v^2}$$

where $v = |\vec{v_1} - \vec{v_2}| = v_1 + v_2$ (provided the particles approach each other at 180^o) is the initial relative velocity of the projectile and target. Here θ is the scattering angle of the reduced mass particle, which as explained above is the scattering angle of the projectile in the CM frame. Substituting equation (3) in (1) yields

$$\frac{d\sigma}{d\Omega} = \frac{a^2}{4}\frac{1}{\sin^4(\frac{\theta}{2})} = (\frac{q_1 q_2}{4\pi\epsilon_0}\frac{1}{\mu v^2})^2\frac{\csc^4(\frac{\theta}{2})}{4} \tag{4}$$

This is the general equation for the differential cross section for a two-particle collision via coulomb interaction in terms of the scattering angle in the CM frame.

4.2 Rutherford scattering

Rutherford scattering is a special case of the general coulomb scattering that has been treated above. It got its name owing to the famous Rutherford's scattering experiment (which was conducted by his students Geiger and Marsden) in which a beam of alpha particles (projectile) were aimed at a stationary thin gold film (target). To derive the equation to model the scattering, Rutherford assumed that the recoil of the gold atom is negligible owing to its greater mass (the gold atom is approximately 50 times more massive than an alpha particle), in essence choosing the target particle to be infinitely massive so that it remains fixed in space. The lab and CM frames are equivalent in this case and this means that the scattering angle is the same in both reference frames. Also, $\mu = m_1$ (since $m_1 << m_2$) and $v = v_1$ (since $v_2 = 0$). Thus we end up with the equation

$$\frac{d\sigma}{d\Omega} = (\frac{q_1 q_2}{4\pi\epsilon_0}\frac{1}{m_1 v_1^2})^2 \frac{\csc^4(\frac{\theta}{2})}{4}$$

4.2.1 Experimental considerations

Before we move on to adding further complexities to this experiment, we shall first take a look at the details of the experimental setup. This is important because a lot of these considerations are also valid for modern high energy experiments that are done in colliders. The first one is regarding the energy imparted to the projectile. It should be such that the wavelength of the projectile and the dimensions of the target are comparable. This is explained in detail in section 5. Also, the experiment was conducted inside a vacuum chamber so that the alpha particles don't lose their energy on collisions with molecules in the air. This is also a characteristic that is shared by modern colliders. Another important aspect of such experiments is how the deflected particles are detected. In this experiment, they used a zinc sulphide screen, which would emit light when hit by an alpha particle, and they manually counted the number of incident particles. Modern experiments employ a variety of such detectors, depending on the type and energy of the particles to be detected. The target used was a thin gold foil. Gold was used because it is a very ductile metal, which meant that it could be made into very thin sheets. This was necessary as a thin sheet would increase the probability that the alpha particles don't undergo multiple collisions.

4.2.2 Projectile beam with constant velocity

If instead of a single projectile particle, we have a projectile beam with intensity Q and the target is now a film of number density n and thickness t, then the number of particles scattered per unit solid angle at an angle θ is given by [4]

$$y = ntQ \cdot \frac{d\sigma}{d\Omega} = [(\frac{1}{4\pi\epsilon_0}\frac{q_1}{m_1 v_1^2})^2 Q] \cdot [ntq_2^2] \cdot [\frac{\csc^4(\frac{\theta}{2})}{4}] \tag{5}$$

This is the famous Rutherford's scattering equation. The equation has been split into three parts, where the first part represents the contribution of the projectile beam properties, the second of the target properties and the third of the measurement or detection property.

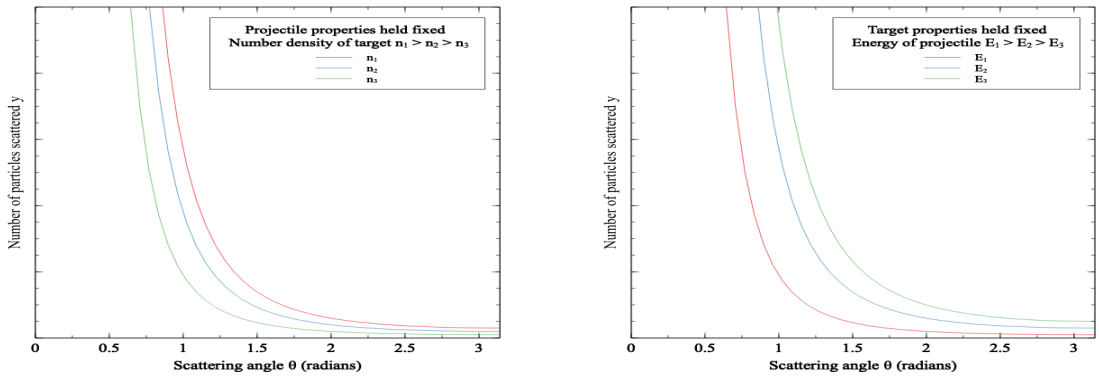

(a) Variation with number density of target particles

(b) Variation with energy of incident particles

Figure 3: Variation of y vs θ with projectile and target properties

4.2.3 Projectile beam with Gaussian velocity distribution

Now we consider the case where all the particles in the projectile beam do not have the same velocity, but is instead distributed randomly about a mean velocity v_0 with a standard deviation σ. We assume the velocities are distributed in the form of a Gaussian curve with the above mentioned values for mean and standard deviation, and then solve for y. This is an approximation of real emitters of particles, for while the Guassian is defined everywhere on the real line, in reality the velocities of projectiles will be bounded by 0 on one end and c (the velocity of light) on the other. The probability density function of the velocity is now given by

$$P(v_1) = \frac{1}{\sigma\sqrt{2\pi}} \exp\{\frac{-(v_1 - v_0)^2}{2\sigma^2}\}$$

As we now need to model the situation where the velocities are spread about a mean, equation (5) needs to be modified. It needs to be multiplied by the probability that a particle has velocity v_1, and then integrated over the whole range of allowed velocities (an underlying assumption here is that the range of velocities is small enough such that the probability of interaction is the same for the whole range). Thus we have

$$dy = \frac{K}{v_1^4} \cdot \frac{1}{\sigma\sqrt{2\pi}} \exp\{\frac{-(v_1 - v_0)^2}{2\sigma^2}\} dv_1$$

where all the terms except v_1^{-4} in equation (5) have been absorbed into K.

$$y = \int_{-\infty}^{\infty} dy = \frac{K}{\sigma\sqrt{2\pi}} \cdot \int_{-\infty}^{\infty} \frac{1}{v_1^4} \exp\{\frac{-(v_1 - v_0)^2}{2\sigma^2}\} dv_1$$

This integral is not analytically solvable. So we first change the limits to finite values, which we choose to be $v_0 - 3\sigma$ to $v_0 + 3\sigma$ (since it would encompass 99.7% of all particles in the Gaussian distribution), and then the resultant integral can be solved numerically. An explicit closed form of this integral could not be obtained, but an attempt was made to determine the dependence of y on the mean velocity v_0 and standard deviation σ. This was done by calculating y for different values of v_0 and σ, plotting those points and then finding the best fit function by least square regression. y was found to be inversely proportional to the fourth power v_0. The fit for the plot y vs σ was less conclusive, and the best fit that was found was $y \propto \frac{e^\sigma}{\sigma}$, although it is likely that it may be a more complicated dependence on σ. However, the general trend is that y increases with increasing σ. These are depicted in figure 4.

5 Incorporating wave nature of particles

Just as all waves have particle nature, all particles have wave nature, which was first conceived by de-Broglie. Thus for any particle with mass m, momentum p and kinetic energy E, its wavelength is given by the equation

$$\lambda = \frac{h}{p} = \frac{h}{\sqrt{2mE}}$$

where h is planck's constant. While the wave nature of everyday objects can be neglected owing to their high masses and slow speeds, this character plays an important role in determining the outcomes of processes involving atomic and subatomic particles that move with high velocities, which is the case for scattering experiments like those that have been studied in this article.

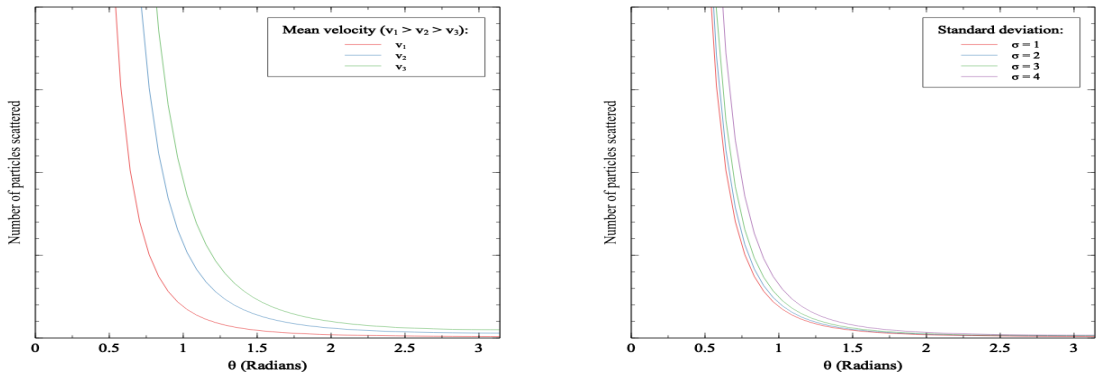

(a) Dependence on mean velocity of velocity distribution

(b) Dependence on standard deviation of velocity distribution

Figure 4: Dependence of y on the properties of velocity distribution of incident beam

When the equation for differential cross section was derived previously by the classical method, both the projectile and the target were taken to be point charges with no wave character. However, it is important to note that the de-Broglie wavelength of the projectile should be comparable to the size of the target particle for interaction to happen. This should be kept in mind when designing scattering experiments. For example, in Rutherford's original experiment, the wavelength of alpha particles used (which had kinetic energy in the low MeV range) was of femtometer order while the diameter of the nucleus of gold atom is 14 fm [5]. Both are of the same order, and so in this case equation (5) provided an accurate fit for the experimental results.

Table 1 shows the de-Broglie wavelength of the electron, proton, α particle and lead atom for the range of kinetic energies 10eV - 100TeV. Given a target particle of specific dimensions, this table can be used to determine which projectile particle to use and with what energy. For example, if we wanted to probe the properties of a gold atom as in Rutherford's experiment (diameter of gold nucleus is 14fm), then as projectiles we could use an electron, proton, alpha particle or lead atom with energies in the neighbourhood of 5 GeV, 5 MeV, 1 MeV or 10 keV respectively.

6 Scattering Amplitude and Form Factor

The scattering amplitude f is an important parameter that arises in the quantum mechanical treatment of the scattering problem. In this view, if the projectile before and after scattering are represented by two different wavefunctions, the scattering amplitude f is a factor by which the amplitude of the scattered projectile gets modified, and is a function of the polar angle θ and the azimuthal angle ϕ. If the target particle possesses azimuthal symmetry, f is independent of ϕ and is a function of θ only. The scattering amplitude is a quantity of interest because the differential cross section is proportional to its square, and in the case of elastic scattering, is exactly equal. ie,

$$\frac{d\sigma}{d\Omega}(\theta) = f(\theta)^2 \tag{6}$$

Given a scattering phenomenon, while the exact calculation of the scattering amplitude is cumbersome, it can be simplified by a method know as the Born approximation [6]. Using this method, the scattering amplitude can be calculated, and the differential cross section for the scattering of an electron off a target of charge Ze (as an example) can be written as

Table 1: Wavelengths of particles for different energies

Energy	Electron (nm)	Proton (A^o)	α particle (A^o)	Lead (A^o)
10 eV	$3.9{\cdot}10^{-1}$	$9.1{\cdot}10^{-2}$	$4.5{\cdot}10^{-2}$	$6.3{\cdot}10^{-3}$
50 eV	$1.7{\cdot}10^{-1}$	$4.1{\cdot}10^{-2}$	$2{\cdot}10^{-2}$	$2.8{\cdot}10^{-3}$
100 eV	$1.2{\cdot}10^{-1}$	$2.9{\cdot}10^{-2}$	$1.4{\cdot}10^{-2}$	$2{\cdot}10^{-3}$
500 eV	$5.5{\cdot}10^{-2}$	$1.3{\cdot}10^{-2}$	$6.4{\cdot}10^{-3}$	$8.9{\cdot}10^{-4}$
1 keV	$3.9{\cdot}10^{-2}$	$9.1{\cdot}10^{-3}$	$4.5{\cdot}10^{-3}$	$6.3{\cdot}10^{-4}$
5 keV	$1.7{\cdot}10^{-2}$	$4.1{\cdot}10^{-3}$	$2{\cdot}10^{-3}$	$2.8{\cdot}10^{-4}$
10 keV	$1.2{\cdot}10^{-2}$	$2.9{\cdot}10^{-3}$	$1.4{\cdot}10^{-3}$	$2{\cdot}10^{-4}$
50 keV	$5.5{\cdot}10^{-3}$	$1.3{\cdot}10^{-3}$	$6.4{\cdot}10^{-4}$	$8.9{\cdot}10^{-5}$
100 keV	$3.9{\cdot}10^{-3}$	$9.1{\cdot}10^{-4}$	$4.5{\cdot}10^{-4}$	$6.3{\cdot}10^{-5}$
500 keV	$1.7{\cdot}10^{-3}$	$4.1{\cdot}10^{-4}$	$2{\cdot}10^{-4}$	$2.8{\cdot}10^{-5}$
1 MeV	$1.2{\cdot}10^{-3}$	$2.9{\cdot}10^{-4}$	$1.4{\cdot}10^{-4}$	$2{\cdot}10^{-5}$
5 MeV	$5.5{\cdot}10^{-4}$	$1.3{\cdot}10^{-4}$	$6.4{\cdot}10^{-5}$	$8.9{\cdot}10^{-6}$
10 MeV	$3.9{\cdot}10^{-4}$	$9.1{\cdot}10^{-5}$	$4.5{\cdot}10^{-5}$	$6.3{\cdot}10^{-6}$
50 MeV	$1.7{\cdot}10^{-4}$	$4.1{\cdot}10^{-5}$	$2{\cdot}10^{-5}$	$2.8{\cdot}10^{-6}$
100 MeV	$1.2{\cdot}10^{-4}$	$2.9{\cdot}10^{-5}$	$1.4{\cdot}10^{-5}$	$2{\cdot}10^{-6}$
500 MeV	$5.5{\cdot}10^{-5}$	$1.3{\cdot}10^{-5}$	$6.4{\cdot}10^{-6}$	$8.9{\cdot}10^{-7}$
1 GeV	$3.9{\cdot}10^{-5}$	$9.1{\cdot}10^{-6}$	$4.5{\cdot}10^{-6}$	$6.3{\cdot}10^{-7}$
5 GeV	$1.7{\cdot}10^{-5}$	$4.1{\cdot}10^{-6}$	$2{\cdot}10^{-6}$	$2.8{\cdot}10^{-7}$
10 GeV	$1.2{\cdot}10^{-5}$	$2.9{\cdot}10^{-6}$	$1.4{\cdot}10^{-6}$	$2{\cdot}10^{-7}$
50 GeV	$5.5{\cdot}10^{-6}$	$1.3{\cdot}10^{-6}$	$6.4{\cdot}10^{-7}$	$8.9{\cdot}10^{-8}$
100 GeV	$3.9{\cdot}10^{-6}$	$9.1{\cdot}10^{-7}$	$4.5{\cdot}10^{-7}$	$6.3{\cdot}10^{-8}$
500 GeV	$1.7{\cdot}10^{-6}$	$4.1{\cdot}10^{-7}$	$2{\cdot}10^{-7}$	$2.8{\cdot}10^{-8}$
1 TeV	$1.2{\cdot}10^{-6}$	$2.9{\cdot}10^{-7}$	$1.4{\cdot}10^{-7}$	$2{\cdot}10^{-8}$
5 TeV	$5.5{\cdot}10^{-7}$	$1.3{\cdot}10^{-7}$	$6.4{\cdot}10^{-8}$	$8.9{\cdot}10^{-9}$
10 TeV	$3.9{\cdot}10^{-7}$	$9.1{\cdot}10^{-8}$	$4.5{\cdot}10^{-8}$	$6.3{\cdot}10^{-9}$
50 TeV	$1.7{\cdot}10^{-7}$	$4.1{\cdot}10^{-8}$	$2{\cdot}10^{-8}$	$2.8{\cdot}10^{-9}$
100 TeV	$1.2{\cdot}10^{-7}$	$2.9{\cdot}10^{-8}$	$1.4{\cdot}10^{-8}$	$2{\cdot}10^{-9}$

$$\frac{d\sigma}{d\Omega} = (\frac{Ze^2}{4\pi\epsilon_0}\frac{1}{m_1 v_1^2})^2 \frac{\csc^4(\frac{\theta}{2})}{4} \cdot |F|^2 \tag{7}$$

where the quantity

$$F = \int e^{\frac{i\vec{q}\cdot\vec{r}'}{\hbar}} \rho(\vec{r}') d^3\vec{r}' \tag{8}$$

is known as the form factor [7]. It depends on the parameters $\vec{q}$ = momentum transfer vector (initial - final momentum of the projectile), $\hbar$ = reduced planck's constant and ρ = spatial charge density of the target (the target is no longer treated as a point charge). The integration is carried out over the whole space. On inspecting equation (7), the following relation becomes apparent:

$$\frac{d\sigma}{d\Omega}(\text{for extended target}) = \frac{d\sigma}{d\Omega}(\text{for point target}) \cdot |F|^2$$

From equation (8), it is seen that the form factor is the Fourier transform of the spatial density distribution of the target. This means that if we know or find the differential cross section, working backwards we can find the form factor, and then taking its inverse Fourier transform will yield ρ. This is a powerful tool that is often used in high energy physics to find

the spacial charge or mass distributions of target particles, and this makes the form factor an extremely useful quantity.

7 Fundamental Forces

Here we take a quick look at the fundamental forces in nature with a particular emphasis on the strong nuclear force. It is important to understand the nature of the forces, their strengths and the kind of particles they act on in order to gain a deeper knowledge of the universe, and of particular interest to us is how they bind the basic building blocks of nature into the matter that we know and see.

According to the standard model of particle physics, which is the theory which explains all the forces except the gravitational force, broadly there are two types of fundamental particles in the world - fermions and bosons. The fermions are the particles which make up all of matter, while bosons are force carriers. This model sees forces as a consequence of particles (fermions) exchanging other particles (bosons).

7.1 Gravitational and electromagnetic forces

The gravitational force and the electromagnetic force acts between particles possessing mass and charge respectively. Both these forces are inversely proportional to the square of the separation between particles. This then implies that both these forces have infinite range, ie, the effect of these forces can be felt over large distances. The force-carrying particle for the electromagnetic force is the photon, while for gravitational force it is thought to be a graviton, whose existence has not yet been proved. The coupling constant of electromagnetic force is about 10^{-2} while that of gravitational force is 10^{-39}, where the coupling constant of a force is a number which signifies its strength.

7.2 Weak nuclear force

The weak nuclear force is the force responsible for radioactivity. For weak interaction, fermions exchange three types of force carriers known as the W^+, W^- and Z bosons. These are extremely massive particles (with masses far greater than that of the neutron) and they decay fast, which is why weak force is an extremely short range force. At distances about a thousandth the radius of a proton (of order $10^{-18}m$), the weak force is about as strong as the electromagnetic force, but then decays exponentially as the distance increases. The weak interaction has a coupling constant between 10^{-6} and 10^{-7}.

7.3 Strong nuclear force

The strong nuclear force is the force that binds quarks inside protons and neutrons (which are collectively called hadrons) and hadrons inside nuclei of atoms. It depends on a property of quarks known as color, which are of types red, green and blue (and their corresponding anti-colors). The force-carrying particle is the gluon. Unlike the electromagnetic force where the photon contains no charge, the gluon contains color, which means that they themselves interact by strong force. This makes the strong interaction a much more complicated force to model than the electromagnetic force. The coupling constant of strong nuclear force is 1, which makes it the strongest of all forces.

The exact dependence of the force on the distance of separation is a rather complicated function, but the following property is of interest. The strong force between two quarks, for example, is at its strongest when the separation between them is slightly less than 1 fm. As the separation increases or decreases from this distance, the strength of the force wanes. This

property is of immense consequence, as we shall see later when we look at the formation of quark-gluon plasma. The strength also decreases with increasing temperature. Thus the interaction between quarks decreases as either temperature or density increases.

8 Phases of Matter and Phase Transitions

A phase is a region of space throughout which all physical properties of a material are uniform [8]. Physical properties a material include not only variables such as pressure and temperature, but also parameters such as the chemical composition. This is different from a state of matter, which is a form in which matter can exist, such as solid, liquid, gas or plasma. To illustrate the difference between the two, consider the example of oil and water at room temperature. Both these materials are in the same state (liquid), while their phases are different because their chemical compositions are not the same. However, both these terms may be used interchangeably when a single material is being observed.

A material that has changed from one phase to another is said to have undergone a phase transition. An example is the phase transition of solid to liquid or liquid to gas. Phase transitions involve changes in the various properties of a system which are often abrupt, though this is not always the case. Phase transitions can be classified in multiple ways based on different characteristics, but it is illuminating to first look at a phase diagram.

8.1 Phase diagrams

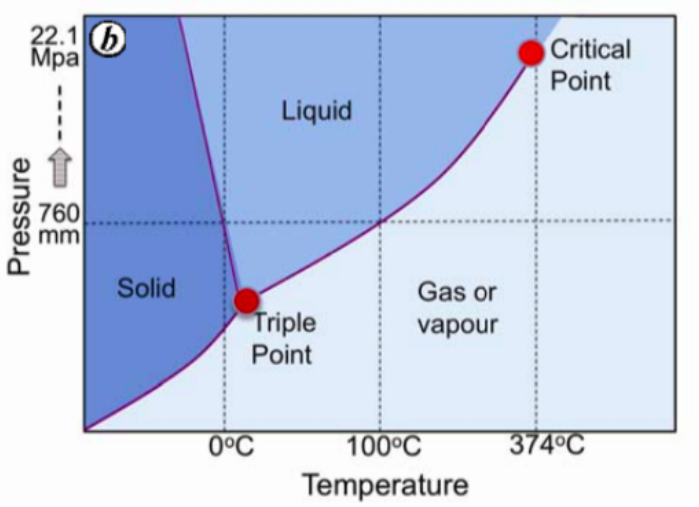

Figure 5: Phase diagram of water [9]

Figure 5 shows the phase diagram of water. The regions marked solid, liquid and gas represent the phases in which water exists at points (which represent a particular value of pressure and temperature) in those regions. The lines separating two phases are known as phase lines, and points on phase lines mark points where water may exist in two or more phases at once. For example, if we chose a point on the phase line connecting the points labelled as triple point and critical point, it represents a boiling point of water, and we know that water may exist as both liquid and gas at its boiling points. At the point where the three phase lines meet, known as the triple point, all three phases of water can exist in equilibrium.

Another characteristic of the phase diagram is the critical point. A critical point in general is any point where a phase line terminates. As a phase line is used to separate two phases, this

means that beyond the critical point, the two phases that were distinguishable earlier now become one. In this specific example of water, the phase line which ends at the critical point separates the liquid and gas phases. As a result, above the critical point the two phases are no longer distinct, and the resulting phase is called supercritical fluid. If a phase transition from liquid to gas phase of water is carried out by a path that goes around the critical point, the phase transition is 'smooth', in the sense that the liquid slowly transforms into gas without any abrupt change in its properties, visible or otherwise. On a separate note, notice that the phase line of the solid-liquid transition of water has a negative slope. This is owing to the fact that the solid state of water (ice) is less dense than its liquid state, which is an anomaly in nature. Therefore in general, this phase line will tend to have positive slope for most materials.

Phases can be differentiated in terms of the symmetries they possess. Typically, a higher phase (one of higher temperature) will have more symmetries, and phase transitions may involve symmetry breaking, which means that symmetries are lost during the process.

8.2 Order parameter

A quantity called the order parameter is often used in relation to phase transitions. Simply put, an order parameter is a quantity whose values differ for two phases in a phase transition and so can be used to tell them apart. For example, density is an order parameter for a liquid-gas phase transition, for it takes values in separate ranges for both these phases. The order parameter is usually expressed in a way such that it is 0 for one phase and 1 for the other, although in real cases it may not exactly equal these values. Above the critical point, the density of liquid and gas become the same. So the difference between the two phases disappears.

8.3 Classifications of phase transitions

A general classification that is used in phase transitions is classification on the basis of order. Given a system, it tries achieve a state with the lowest possible free energy. A closed system which exchanges only energy with its surroundings will minimize its Helmholtz free energy, while an open system which exchanges both mass and energy with its surroundings will minimize its Gibb's free energy. The derivatives of the free energy of the phase with respect to temperature and pressure give rise to meaningful quantities of physical significance. These quantities may not be continuous over the transition. As per Ehrenfest's criteria, an 'n'th order phase transition corresponds to a discontinuity in the 'n'th derivative of the free energy functions. The quantity in which the discontinuity exists is then taken to be the order parameter for the phase transition.

For a first order transition, the entropy S and volume V (and hence the density) which are the first derivatives of free energy (with respect to temperature and pressure respectively) functions exhibit discontinuities. This is why density is often chosen as an order parameter for first order transitions. They are generally abrupt and involve the absorption or emission of latent heat. For first order transitions, the second derivatives of free energy functions, such as the specific heat capacity, diverge at the point of phase transition. An example is that during the phase transition of water to ice, the temperature of water remains constant no matter how heat you apply, until all of the water turns into steam. This implies an infinite specific heat capacity during the phase transition process.

For a second order phase transition, there is no discontinuity either in entropy or volume. Hence there is no latent heat involved in the process. However, the second derivatives of free energies will have finite discontinuities or logarithmic divergence.. An example of an order parameter for second order phase transitions is the specific heat capacity.

A transition which takes place above the critical point is known as a crossover transition. The liquid to vapour transition of water above the critical point is an example for crossover transition.

Further, phase transitions can also be classified as continuous or discontinuous based on the variation of entropy with temperature. First order transitions are thus discontinuous, and second order and above are continuous.

9 Quark-Gluon Plasma

9.1 Introduction

Our search for fundamental particles have led us to understand that atomic nuclei are made of nucleons (protons and neutrons), which are themselves made of quarks. Quarks in nature always stick together because of the strength of the strong nuclear force, and this is called confinement. This nuclear or hadronic matter (matter inside nuclei), is found to be behave like a fluid. It may be liquid or gas like depending on the temperature, and this liquid-gas phase transition of nuclear matter is expected to be a first order transition involving latent heat. Now, when discussing the fundamental forces, we had come across a property of the strong force which renders it weaker on decreasing inter-particle distance or increasing the temperature. This property is called asymptotic freedom. Therefore on either compressing the matter till the hadrons overlap or heating it to extreme temperatures, the strength of the color force decreases to a point where the quarks become free, or deconfined. It results in the formation of a 'soup' of quarks and gluons. This new phase of matter is called the quark-gluon plasma.

The early universe is thought to have been in this phase a short time after the big bang, before matter expanded and cooled down enough for the strong force to come into play and bind the quarks into hadrons. Hence the study of quark-gluon plasma is important if we are to understand the evolution of our universe, and it is expected that it will shed light on a host of other fundamental properties of matter and forces. QGP is also thought to exist inside neutron stars, whose high density would lead to deconfinement of quarks.

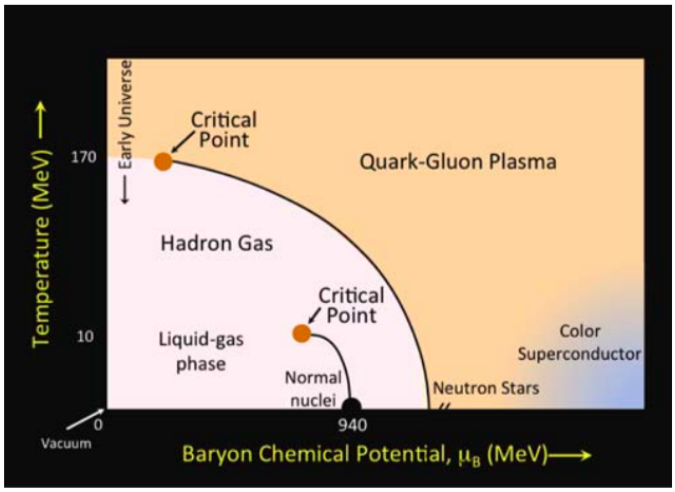

Figure 6: Phase diagram of nuclear matter [9]

Figure 6 shows a phase diagram for nuclear matter. The quantity on the x-axis, the baryon chemical potential (baryons are composite particles such as protons and neutrons

that are made up of an odd number of quarks) is the energy needed to add an additional quark to the existing matter, and can be thought of as the net baryon count in the system (or equivalently as baryon density). Note that at high temperatures and/or high densities, matter exists in the QGP phase. In the early universe, the net baryon count was low (as the number of baryons and anti-baryons was almost equal) and the temperatures were very high. As the universe cooled and the baryon count went up, matter underwent hadronization (the process of quarks forming hadrons), and then subsequently hadrons came together to the nuclei of atoms that we know of. There are two phase lines - between the liquid and gas phases of hadrons, and between hadron gas and quark-gluon plasma. The critical points are thought to exist, although they have not been experimentally observed.

Because of the intense pressures and temperatures needed to form QGP, only in the early 21st century did we gain the technological capability to produce QGP artificially, with the advent of modern high-energy heavy-ion colliders such as the Relativistic Heavy Ion Collider (RHIC) at the Brookhaven National Laboratory (BNL) and the Large Hadron Collider (LHC) at CERN. When heavy ions (gold at RHIC and lead at LHC) are accelerated to high energies and then made to collide with each other, a fireball of extreme density and temperature is formed, in which quarks undergo de-confinement and QGP is formed. This system is then thought to develop in the same way our universe did after the big bang. While the QGP itself cannot be observed directly (for it is extremely short lived), finding the distributions and energies of the hadrons (which form when the QGP undergoes hadronization) along with those of other kinds of particles that are emitted in the collision, and using various 'probes', different properties of QGP can be studied, utilizing the help of a suitable theoretical model for the collisions. The STAR and PHENIX experiments at RHIC and the ALICE experiment at CERN work in the above explained manner.

9.2 Phase transition from hadronic phase to QGP

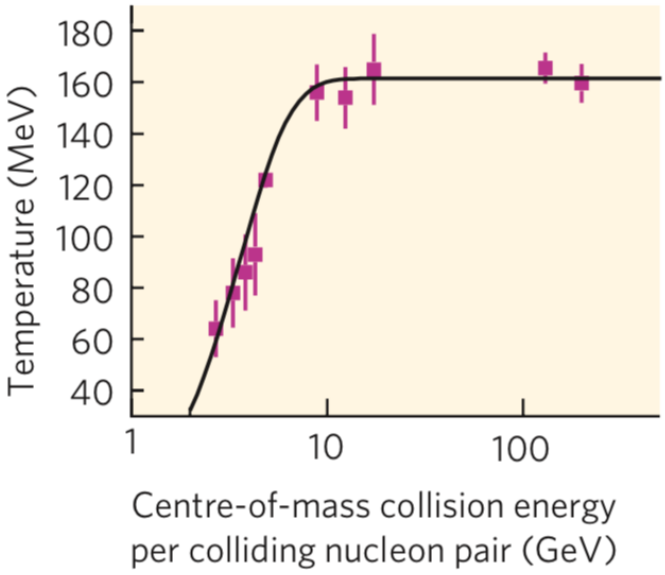

Figure 7: Plot of collision energies vs temperature of out-going hadrons [10]

Before we delve deeper into the theoretical aspects of QGP and its various properties, it is important to understand how is it that we know that hadron gas undergoes a phase transition, and what kind of phase transition it is. Figure 7 is a plot of a set of experimental data obtained

from RHIC. The collision energy of incident particles (on the CM frame) is given on the x-axis, and the temperature of the out-coming hadrons is given on the y-axis. Initially, it is seen that the temperature is linearly increasing with the collision energy. However, at about 10 GeV, the curve becomes flat, and the temperature remains constant. This observation has a profound implication. We could use analogue to understand this easily, and the phase transition of water in its liquid phase to vapor will suffice. As long as the temperature of water is below its boiling point, its temperature increases on applying more heat, where heat is analogous to the collision energy, which is nothing but the energy given to the system. If water reaches its boiling point, on the other hand, its temperature stays fixed, and the additional heat applied (the latent heat) is utilized to undergo the phase transition into vapor, and then once the transition is complete, to heat the vapor. A similar reasoning can be applied to explain figure 7.

This and matching observations from other experiments have led us to conclude the following:

1. Hadronic matter appears to undergo a phase transition into a new phase.
2. The temperature for the transition is around 160 MeV.
3. The transition is likely to be a first-order transition because it seems to involve latent heat.

While first and second conclusions are now taken to be true (although the exact transition temperature has not yet been determined), there is considerable debate as to the order of the transition. It turns out that QCD calculations (Quantum Chromodynamics, the theory explaining the interaction of quarks and gluons) involving a finite and non-zero net baryon density are extremely complex to solve even with the help of computers, and this has hindered scientists from putting forward persuading arguments to support one possibility over the others.

9.3 Experimental detection of QGP

As briefly explained above, while the QGP formed in a heavy-ion collision cannot be directly observed, its effects will be visible on looking at different properties of various particles that are generated in such a high energy collision. In this section we look at the two most important experimental observations/phenomena that indicate the formation of QGP.

9.3.1 Jet Quenching

In a heavy ion collision, pairs of quarks and gluons on slamming into each other get scattered back-to-back, which then condense into other particles such as pions and kaons (which are quark-antiquark pairs). These so called 'jets' can be observed and their energies can be measured in a collision experiment.

In a heavy-ion collision carried out at STAR at RHIC in 2003, scientists observed for the first time what is known as jet quenching [12]. It was seen that one of the two back-to-back jets had much lower energy than the other, which had never been observed for collisions involving lighter nuclei and/or lower energies. The reason for this is that the pions and kaons in a jet interact much more strongly with free quarks than hadrons, and hence will loose considerably more energy on interaction. Therefore the further a jet has to travel through QGP, the more energy it loses. Jet quenching is considered to be the first experimental evidence of the formation of QGP.

9.3.2 Elliptic Flow

In a collision of two nuclei, a pressure gradient develops at the time of collision owing to the density distributions of the nuclei. This pressure gradient works to impart an additional momentum to the particles created in the collision in addition to their thermal motions. In a central, head-on collision, this pressure gradient is spherically symmetric. However, if the collision is a peripheral one, where they are separated by a non-zero impact parameter, the collision area and hence the pressure gradient is not radially symmetric. An illustration of this is given in figure 8.

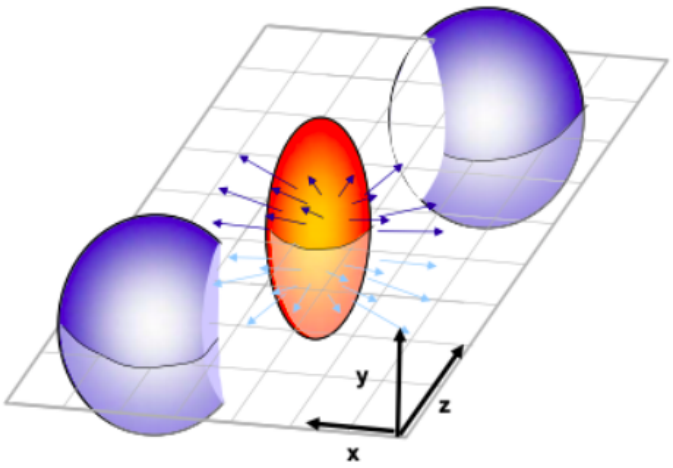

Figure 8: Figure depicting a peripheral collision which shows the participants (interacting nucleons) in red and spectators (non-interacting nucleons) in blue. The reaction plane is the x-z plane in the diagram, which is formed by the impact parameter and the beam direction. [13]

As shown in the figure, the reaction volume is almond shaped or elliptical. As a result the pressure gradient that develops is spatially anisotropic, which manifests itself as an anisotropy in the momentum of the particles that are generated in the collision [14]. In other words, this asymmetry is caused by multiple interactions between the constituents of the created matter and the initial asymmetries in the spacial geometry of a peripheral collision [15]. Simply put, elliptic flow is measure of this azimuthal anisotropy in the generated particles. The magnitude of elliptic flow depends strongly in the friction in the created matter, which is characterised by the ratio shear viscosity to entropy η/s. The anisotropies will only propagate if the matter has low viscosity; In a highly viscous medium, the anisotropies get extinguished. Observations and measurements of elliptic flow in high energy heavy-ion collisions and their subsequent analysis have revealed that the initial matter created in such collisions behaves like a fluid with very low friction, which fits in nicely with our expectation for a plasma.

9.4 Chiral symmetry breaking

Chiral symmetry breaking is a phenomenon that accompanies that transition from QGP to hadron phase. To understand this process, we shall start with the concept of helicity.

The spin of a particle has two possible orientations with respect to its direction of motion - they can be either parallel (facing the same direction) or anti-parallel(facing the opposite direction). The particle is said to be a right-handed particle they're parallel, and left-handed if they're anti-parallel. This property is called the helicity of a particle. it is important to note that helicity in general is not an intrinsic property of a particle, and it may depend on

the frame of reference, because the velocity of a particle is different for two observers who are in relative motion. Therefore helicity is not fixed for a particle, unless the particle is a massless particle which consequently travels at the speed of light, in which case the helicity will be the same for all observers, and hence fixed.

Particles possess another property called chirality, which can be thought of to be an intrinsic analogue of helicity. For a massless particle, chirality and helicity are the same, for as I explained above the helicity for such a particle is fixed. For particles having mass, however, the definition of chirality is a bit more complex. One way to think about it is when you rotate a particle, its quantum wavefunction shifts (a phase is introduced) in different ways depending on whether the particle is right or left handed [16]. The important thing to understand is that chirality is an intrinsic quantum mechanical property of any particle, and this is relevant because nature treats right and left handed particles differently. This is what is meant when people refer to the standard model as a chiral theory. Certain particles may interact or not depending on their chirality.

In QGP phase of matter, the quarks are essentially free, as the interaction between them is small. In this state, they have a very small mass, and right or left handed particles are indistinguishable, in a sense. So we say that chiral symmetry is present in the QGP phase. However, when the quarks combine to form hadrons, the strong interaction contributes to the mass of the hadron (in a way similar to concept of relativistic mass), and the actual term for this is QCD binding energy. As a result, of the total the mass of the proton, for example, only about 1% is the actual contribution from the quarks's rest masses. This is thought to be caused by a loss in chiral symmetry, where the particles now gain a distinct 'handedness'. This process is called chiral symmetry breaking.

10 Conclusion

It has not been 20 years since the first detection of the quark-gluon plasma, and while we have made great progress in unravelling its mysteries, there is still a long way to go. Trying to accurately model the phase transition from hadron to quark matter is one of the biggest theoretical challenges in this field, and experimental hurdles include expanding the range of energies that is currently being probed, which is bounded by our technological limitations. Despite this, the allure of QGP remains unaffected owing to its promise to help us gain insight into the evolution of the universe. This is an exciting and active field of physics, and one that is sure to reap us great rewards in the future.

References

[1] Collisions in plasma [pdf] by MIT. Retrieved from https://ocw.mit.edu/courses/nuclear-engineering/22-611j-introduction-to-plasma-physics-i-fall-2006/readings/chap3.pdf

[2] Rajam, J.B. Atomic Physics . 1950. S. Chand. 7th Edition.

[3] Collisions of charge particles [pdf] by MIT. Retrieved from https://ocw.mit.edu/courses/nuclear-engineering/22-105-electromagnetic-interactions-fall-2005/readings/chap6.pdf

[4] Rutherford, E. The scattering of α and β particles by matter and the structure of the atom. 1911. Philosophical Magazine. 6-21: 669-688

[5] Geiger, H.; Marsden, E. On a Diffuse Reflection of the α-Particles. 1909. Proceedings of the Royal Society A: Mathematical, Physical and Engineering Sciences. Proceedings of the Royal Society. 82 (A): 495?500.

[6] Griffiths, David J. introduction to quantum mechanics. 1995. Prentice Hall.

[7] Foster, Kyle. Electron scattering: Form factors and nuclear shapes [pdf]. Retrieved from http://inside.mines.edu/ kleach/PHGN422/supplemental/eScatteringFormFactors_Supplemental.pdf

[8] Modell, Michael; Robert C. Reid (1974). Thermodynamics and Its Applications. Englewood Cliffs, NJ: Prentice-Hall.

[9] Nayak, Tapan. Phases of nuclear matter. 2012. Current Science. Vol. 103, No. 8.

[10] Braun-Munzinger, Peter. Stachel, Johanna. The quest for the quark-gluon plasma. 2007. Nature. Vol 448.

[11] Harris, John W. Muller, Berndt. The search for the quark-gluon plasma. 1996. Annu. Rev. Nucl. Part. Sci. 1996. 46:71?107

[12] Heavy ions and quark-gluon plasma. Retrieved from https://home.cern/science/physics/heavy-ions-and-quark-gluon-plasma

[13] Elliptic flow measurement at ALICE

[14] van der Kolk, Naomi. To flow or not to flow - A study of elliptic flow and nonflow in proton-proton collisions in ALICE. 2011. Ipskamp Drukkers.

[15] Alice gets with the flow. CERN Courier

[16] https://www.quantumdiaries.org/2011/06/19/helicity-chirality-mass-and-the-higgs/

[17] Rajagopal, Krishna. Free the quarks. 2001. Spring Beeline SLAC.